

# Smartphone-Enabled Paper-Based Hemoglobin Sensor for Extreme Point-of-Care Diagnostics

Sujay K. Biswas, Subhamoy Chatterjee, Soumya Bandyopadhyay, Shantimoy Kar, Nirmal K. Som, Satadal Saha, and Suman Chakraborty\*



Cite This: *ACS Sens.* 2021, 6, 1077–1085



Read Online

ACCESS |

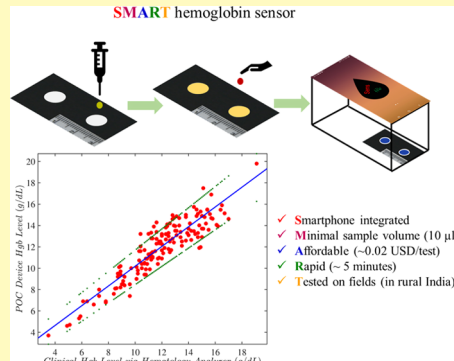
Metrics & More

Article Recommendations

Supporting Information

**ABSTRACT:** We report a simple, affordable ( $\sim 0.02$  US \$/test), rapid (within 5 min), and quantitative paper-based sensor integrated with smartphone application for on-spot detection of hemoglobin (Hgb) concentration using approximately  $10\ \mu\text{L}$  of finger-pricked blood. Quantitative analytical colorimetry is achieved via an Android-based application (Sens-Hb), integrating key operational steps of image acquisition, real-time analysis, and result dissemination. Further, feedback from the machine learning algorithm for adaptation of calibration data offers consistent dynamic improvement for precise predictions of the test results. Our study reveals a successful deployment of the extreme point-of-care test in rural settings where no infrastructural facilities for diagnostics are available. The Hgb test device is validated both in the controlled laboratory environment ( $n = 200$ ) and on the field experiments ( $n = 142$ ) executed in four different Indian villages. Validation results are well correlated with the pathological gold standard results ( $r = 0.9583$ ) with high sensitivity and specificity for the healthy ( $n = 136$ ) ( $>11\ \text{g/dL}$ ) (specificity: 97.2%), mildly anemic ( $n = 55$ ) ( $<11\ \text{g/dL}$ ) (sensitivity: 87.5%, specificity: 100%), and severely anemic ( $n = 9$ ) ( $<7\ \text{g/dL}$ ) (sensitivity: 100%, specificity: 100%) samples. Results from field trials reveal that only below 5% cases of the results are interpreted erroneously by classifying mildly anemic patients as healthy ones. On-field deployment has unveiled the test kit to be extremely user friendly that can be handled by minimally trained frontline workers for catering the needs of the underserved communities.

**KEYWORDS:** POC device, smartphone app, hemoglobin detection, paper-based sensors, colorimetric detection



Anemia, pathologically diagnosed by reduced hemoglobin (Hgb) concentration of blood below a threshold limit, often brings in different complications in physiological and organ functionalities in affected patients.<sup>1,2</sup> Hgb-related disorders create significant global impact on health as 2.36 billion people get affected annually.<sup>3,4</sup> According to the guidelines of the World Health Organization (WHO), the lower thresholds of Hgb are 13 (male), 12 (non-pregnant female), 11.5 (children: age 5–11.9 years), and 11 g/dL (pregnant female and children younger than 5 years).<sup>5</sup> Hgb concentrations below these lower threshold limits may turn out to be of the most detrimental consequence in certain vulnerable sections including pregnant women, children, and immunosuppressed patients. In their broad interests, regular monitoring of hemoglobin concentration is therefore strongly recommended. However, in underserved communities, early diagnosis and frequent monitoring remain to be grossly elusive, primarily attributed to unaffordable and inaccessible centralized healthcare facilities.

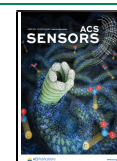
Standard diagnostic protocols for Hgb tests are well established in centralized pathological settings. However, these methods are not well suited for adaptation in point-of-care (POC) applications. In the gold standard practice, blood

hemoglobin is transformed into cyanmethemoglobin using Drabkin's solution for spectrophotometric analysis in a hematology analyzer.<sup>6,7</sup> Significant efforts have been put forward toward developing a low-cost, user-friendly, POC device as a viable alternative to the bulky sophisticated instruments used in conventional laboratories for hematological analysis.<sup>8–20</sup> In this regard, several techniques such as colorimetric detection using 2,7-diaminofluorene, electrochemical detection, luminescence assays, carbon-dot-based fluorescence assays, and so on have been explored for developing sensitive and rapid Hgb estimation assays.<sup>21–26</sup> In the quest of offering improved sensitivities, many of these approaches, however, bring in prohibitive complexities and auxiliary expenses, limiting on-field applications to a large extent. To circumvent these constraints, a portable scanner-based colorimetric detection of Hgb from dried stain of the blood–Drabkin's mixer has been reported.<sup>1</sup> By measuring the

**Received:** November 11, 2020

**Accepted:** January 26, 2021

**Published:** February 26, 2021



absorbance using CMOS sensors, an optical detection technique has also been demonstrated for the estimation of Hgb concentration from calcium-free Tyrode buffer-diluted blood samples in a polydimethylsiloxane (PDMS) microchannel.<sup>27</sup> In a recent work, separation and identification of common hemoglobin variants (A, F, S, and C/E/A2) from lysed blood is reported by exploring the method of paper-based electrophoresis on a portable device.<sup>28</sup>

Reported studies reveal that suitability of a point-of-care device for hemoglobin detection is often compromised with its poor standard of quantitative predictive capability despite some other elusive benefits. As a consequence, these methods have not been proven to be sensitive enough to provide a precise estimation of the Hgb concentration in the transition zone of mild to severe anemic conditions and therefore clinically ineffective when a clear decision needs to be taken on possible measures of exigency including blood transfusion. Such deficits become even more prohibitive in resource-limited settings, where complementary diagnostic facilities to narrow down the clinical decision-making window appear to be scarce.<sup>29,30</sup>

Here, we report an ultra-low-cost, user-friendly, paper-based Hgb sensor integrated with a smartphone app for rapid detection of hemoglobin for high-fidelity diagnostics in underserved settings. Our device demonstrates a ready-to-answer paper-based platform for rapid quantification of Hgb with an expense of ~0.02 US \$ per test on the field. The device utilizes a drop of finger-pricked blood for colorimetric assay (shown in Figure 1A), which is analyzed by a smartphone-based Android app (named as “Sens-Hb”). The results of our device are validated with the results of laboratory-based gold standard protocols. Quantitative predictive capability of the device is enhanced by employing an optimized stoichiometry-driven chemical protocol. The in-house developed smartphone-based Android app is equipped with essential features for image acquisition (within optimized illumination settings) and subsequent analysis using a machine learning algorithm. Furthermore, the “Sens-Hb” app performs pre-processing of acquired images to eliminate undesired noises and normalization of the extracted features to improve the result accuracy. In contrast to other reported POC devices, our device turns out to be cost effective, virtually instrument free, deployable with minimally trained personnel in extreme POC settings, and capable of reproducing gold-standard results. We have tested this prototype first with the participation of 200 volunteers in laboratory settings (venous blood used) and 142 volunteers in the field settings (finger-pricked blood used) across four villages in the state of West Bengal, India. A parallel comparison with a standard hematology analyzer (Sysmex Kx21) and a HemoCueHB-201+ device (considered as an established POC device) reveals that the present device offers supreme accuracy in affordable price. The feedback given by the machine learning algorithm from image processing provides consistent improvement for more precise prediction of the test results as progressively more test data sets are included for training the predictive model via image analytics.<sup>31</sup>

## EXPERIMENTAL SECTION

**Fabrication of the Paper-Strips.** Microfluidic paper strips are fabricated using Whatman (grade 1) cellulose filter paper (mean pore diameter: 11  $\mu\text{m}$ ) by a simple printing-based procedure developed by our group.<sup>32</sup> The manufacturing steps include printing by a simple office printer (HP Color LaserJet 500) using normal cartridge ink, which forms a hydrophobic barrier upon heating at 180 °C for 4–5 min.

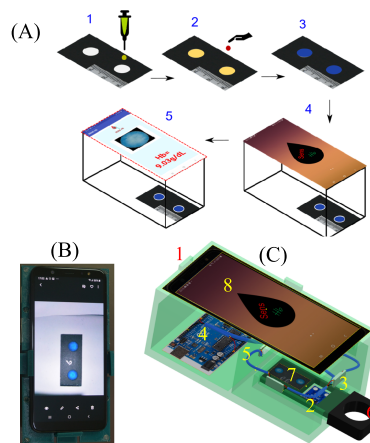


**Figure 1.** (A) Schematic representation of the detection protocol shown stepwise. Five key steps include (1) embedding chemical reagents on the paper device, (2) putting a drop of blood from finger prick, (3) colorimetric changes on the paper device, (4) placement of the device on a cartridge within a customized portable plastic box, and (5) smartphone integration, analytics, and dissemination based on colorimetric signals of the test outcome. For improved performance, prior to step (2), finger-pricked blood is mixed with Drabkin's solution for 15 s before introducing onto the reaction spots. (B) Top-view image of the POC device during the testing of a blood sample. The smartphone app displays two reaction spots of the paper device. A greenish-blue color is developed after the reaction, which is captured by a smartphone. (C) Schematic representation of the present device is shown where the smartphone is placed on top of the 3D box. Key components are (1) sliding bars to fit in different models of smartphone, (2) light intensity-measuring microchip that continuously sends feedback to maintain uniform light intensity, (3) LED light source, (4) Arduino board, (5) cable connections between the Arduino board with a light measurement unit and (6) paper-made cartridge, (7) paper-based reaction spots, and (8) smartphone with the Sens-Hb app.

This fabrication technique is relatively simple and suitable for large-scale manufacturing compared to other popular methods like wax printing<sup>33</sup> and use of modified/specific chemicals.<sup>34–38</sup> Notably, although we use only one reaction spot for the assay, we have designed two identical reaction spots to avoid an unforeseen mishandling, which may occur while performing on-site testing by unskilled personnel, and thereby maximizing the outputs from the field experiments.

**Fabrication of the Plastic Box.** The entire diagnostic process is done in a simple plastic box, which holds the smartphone at the top. The paper strip is inserted into a confined area where a uniform illumination is maintained for image recording (Figure 1C). The plastic box and the paper-strip cartridge are designed in AutoCAD and subsequently 3D printed (TECHB V30) using a PLA (polylactic acid) filament. A rectangular opening at the top surface facilitates the required field-of-view for the inbuilt smartphone camera and a guided slit at the front wall to insert the cartridge with the paper strip, which allows the correct alignment with the camera. The top part of the box houses an arrangement for horizontal movement to accommodate any smartphone with its camera at a fixed position just above the reaction pad. The distance between the mobile camera and reaction pad has been optimized based on the minimum focal length of the camera lens. Constant light illumination on the paper platform is maintained by setting up mobile phone USB-powered LED light (12–15 mW) in the inner cavity of the plastic casing. A constant current supply to the LED is ensured by a PNP transistor circuit and an Arduino microcontroller enabled pulse width modulator. A micro-lux meter chip is integrated for sensing the light intensity on the region of interest (ROI).

**Mobile App (Sens-Hb) Development.** Sens-Hb, an Android-based mobile application, is developed for executing three essential functionalities of the quantitative diagnostic assay: image acquisition with pre-defined time interval, image processing and analysis, and

display of the test results (illustrated in Figure 2). In parallel, the app receives feedback from the pre-installed microsensor (within the plastic

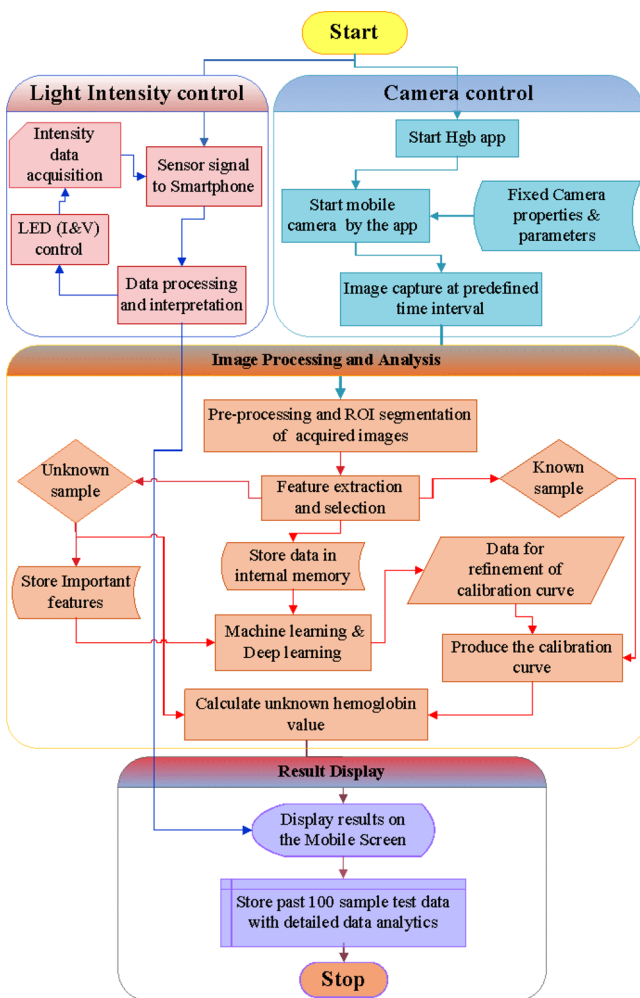


**Figure 2.** Flowchart of the “Sens-Hb” app. Four key functions include (a) controlling camera properties and (b) light intensity, (c) image acquisition and post-processing, and (d) result display. The function for controlling the mobile camera invokes the desired camera properties, which are hardcoded in the internal memory. Captured images are stored in the internal memory and read by the image processing module for feature extraction and analysis. Dynamic adaptation of the calibration curve is based on the new calibration results obtained through machine learning analysis. The app maintains the uniform light condition by controlling the current and voltage of the LED after receiving the feedback from the installed micro-chip about the lux intensity.

casing) to adjust the light illumination on the reaction pad as per the desired lux intensity. Camera properties for image recording such as mode, ISO, white balance, exposure time, shutter speed, and so on are optimized and hardcoded in the algorithm in a separate function. A timer function is set within the app to trigger the mobile camera for image recording at the specified time interval of 120–240 s (based on the optimized colorimetric chemical assay). After acquisition, these images are processed in four sequential stages: pre-processing (white balance adjustments, light gradient corrections, and elimination of color masking), segmentation of ROI (i.e., precise identification of colorimetric signals irrespective of variations), extraction of image features, and finally analysis of the extracted features to estimate the Hgb value by invoking the calibration curve. Additionally, these image features are sent for machine learning analysis to assess and minimize the gap between extracted results and calibration set data points by real-

time adaptation of the calibration curve. The segmentation process precisely identifies the essential area of the colored region by combining the threshold, region, and color-based segmentations techniques, irrespective of the color intensity variations across the circular reaction pad. The underlying colorimetric assay delineates fast and significant alternations in R and B values in the RGB color space. These image features have been accounted during analysis and thereby given due weightage in the mathematical formulations. Furthermore, a separate function block on machine learning-based data analysis for dynamic and continuous adaptation of the calibration curve has also been included. The step-wise operation of the mobile app for the entire detection process is shown in the Supporting Information, Figure S1.

#### Optimization of Colorimetric Assay and Device Calibration.

First, the device is calibrated with different concentrations of standard cyanmethemoglobin (equivalent to standard hemoglobin) after making the serial dilution using Drabkin’s solution (SPAN Diagnostics Ltd.). To perform the assay on a paper device, 10 μL of blood is mixed with Drabkin’s solution in a volumetric ratio of 1:250 (v/v %) prior to introduction on the hydrophilic reaction pad of the paper device. The hydrophilic reaction zones are pre-wetted with 2 μL of the chromogenic reagent (*o*-tolidine (98% AR, LOBA Chemie, India), concentration: 400 mg/dL) (for details, please see the Supporting Information). The device is first tested in controlled laboratory settings with 200 venous blood samples and subsequently in field settings with 142 finger-prick blood samples, covering a wide spectrum of Hgb levels. The step-wise details of the colorimetric assay are summarized in Figure 1A. Further, to eradicate any bias of using a specific phone camera, we have captured the images using three different smartphones, namely, Samsung Galaxy A6 plus, Google Pixel 3, and Nokia 6, incurring negligible differences in the quantified predictions of the test results.

**Image Processing.** Acquired images are processed using the in-house developed algorithm on an Android platform. The Sens-Hb app starts image recording between the specified time window of 120–240 s, with image selection in every 15 s interval followed by processing of these selected images and subsequent display of Hgb result on the mobile screen without requiring any intermediate interventions from the users. A specific time window of 120–240 s is considered for image recording based on the experimental observation for completion of the colorimetric reaction. After elimination of the undesired noises, the ROI is identified by the process of segmentation to extract the image features (e.g., grayscale intensities and RGB values). To eradicate the fluctuations related to focusing magnification and illumination, a linear transformation has been adapted to convert all the black and white region to the equivalent grayscale value of 0 and 255, respectively. The subscripts “R” and “UR” denote the image features corresponding to the reacted and unreacted reaction pads, respectively. Image features of the reaction pad, wetted with the chromogenic reagent before the onset of the chemical reaction ( $I_{UR}$ ), are first calculated and linearly transformed. Dynamic variation of intensity of the reaction pad during the chemical reaction is explicated and discussed later in the section titled “Image Processing Algorithm”. Temporal average of the image features ( $I_{R,MAX}$ ) within the intended time, after the completion of chemical reaction, is subsequently obtained and scaled accordingly. Difference of intensities ( $\Delta I$ ), corresponding to a given concentration, are obtained by:

$$\frac{\Delta I}{255} = \frac{I_{R,MAX} - I_{BR}}{I_{WR} - I_{BR}} - \frac{I_{UR} - I_{BUR}}{I_{WUR} - I_{BUR}} \quad (1)$$

**Image Processing Algorithm.** Smartphone-based image analytics involves four key steps: (I) selection of region of interest (ROI) and segmentation, (II) feature extraction, (III) regression, and (IV) training of the algorithm, which are followed subsequently.

- I. Region of interest (ROI) selection. Precise selection of the region of interest (ROI) from the captured image is most essential for obtaining accurate results in the downstream processes. However, accurate identification of the ROI is a challenge due to non-uniform color generation across the reaction pad along with variation in patterns from image to image. This problem has been addressed by sequentially

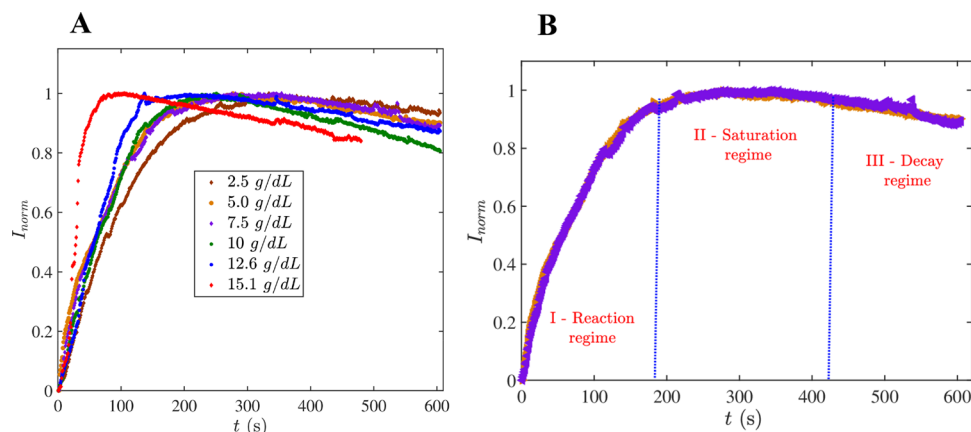


**Figure 3.** Reaction kinetics of chemical assay: (A) reaction kinetics of the cyanmethemoglobin solution with Hgb levels of 2.5, 5.0, 7.5, 10.0, 12.6, and 15.1 g/dL. A sharp decrease in reaction completion time is seen with an increasing Hgb concentration. (B) Temporal variations of normalized intensity ( $I_{norm}$ ) unveil three distinct regimes of the assay: normalized intensity maxima lie in regime II (orange- and magenta-colored curves represent 5.0 and 7.5 g/dL, respectively).

employing the color-based thresholding, Otsu's global thresholding, and region-based method to ensure the correct identification of the desired ROI from the images subjected to analysis.

**II. Feature Extraction.** Development of a non-uniform colorimetric signal seems to be one of the inherent issues that often brings further challenges in the post-processing steps. Background color and texture of the paper add further complexities, particularly during extraction of the feature characteristics. In this context, we use a min–max normalization technique on the mean color intensity (RGB) extracted from the ROI. Non-uniformity of the color channels is normalized and then considered for extracting relevant statistical features. The white balance and contrasts are corrected by considering two reference images of white and black. Furthermore, a statistical feature selection algorithm, namely RReliefF,<sup>39</sup> is used to identify the most significant secondary features strongly correlated to the physiochemical change of the colorimetric reaction.

To eradicate the manual interventions while selecting the statistical features, we use an iterative rank assignment RReliefF algorithm on the desired features.<sup>40–42</sup> This algorithm assigns weightage on the selected features by monitoring the continuous change of the dependent variables (i.e., hemoglobin concentration in our case) from the entire set of variables. It works based on the principle of penalizing the features with a large distance with the nearest response values while awarding the features with a negligible distance with the nearest response values (for more details, please see the Supporting Information).

**III. Regression analysis.** The regression analysis method uses the extracted features and hemoglobin concentration as independent and dependent variables, respectively, to make the best prediction. Furthermore, we adapted a dynamic revision of the regression algorithm as new experimental data are available through a convex optimization process.

**IV. Training of the algorithm.** We have trained our algorithm by testing with a large number of experimental images (>1000 images) obtained for blood samples with known Hgb values. Experimental images for both the venous and finger-pricked blood samples are used for training of the algorithm. An iterative 10-fold operation has been implemented to overcome the bias and overfitting of real-time data. In this procedure, 90% of the experimental images are considered for the gradient descent training to find the optimal regression equation while the rest of the 10% is considered for validation of the algorithm. In the subsequent step, the images considered for validation in the previous step are included in the training set, while another 10% is picked up from the previous training set for new validation.

This cross-check operation is repeated 10 times to ensure that there are no overlapping training and validation data set.

For each iteration, a new regression curve is compared to the previous iteration and found to be minimally varying, which reflects no overfitting during the iterative process. The overall regression equation is quantified by the average over 10-fold operations. From the validation results, it is evident that mean square error for 10-fold operations is minimal, which manifests the higher predictive accuracy of our systems.

**Statistical Analysis.** To obtain the statistical relevance of the experimental outcomes, we have explored both supervised and unsupervised machine learning approaches in our algorithm for pre-processing, regression analysis, and real-time dynamic adaptation. Pearson correlations, linear regression models, and the ratio of the mean and prediction bounds are employed to estimate the correlation between Hgb levels via a pathological hematology analyzer (Sysmex Kx21), Hemocue (HB-201+), and POC device. Sensitivity and specificity results are determined collectively for the volunteers irrespective of their age, sex, and ethnicity.

**Study Approval and Sample Collection.** An approval of ethical clearance was taken from the Institute Ethical Committee (IEC no. IIT/SRIC/DR/2017) for the commencement of this study. Blood samples were collected during the period of 2017–2020 as part of routine diagnostics of anemia at the pathology clinic of the B.C. Roy Technology Hospital, Indian Institute of Technology Kharagpur. The POC device was validated with 200 venous blood samples, including severely anemic ( $n = 9$ ), mildly anemic ( $n = 55$ ), and healthy ( $n = 136$ ) patients. Further, validation of the device with finger-pricked blood ( $n = 142$ ) was performed in four field trials organized in rural India in the state of West Bengal devoid of even very basic infrastructure for laboratory testing (Supporting Information, Figure S3). All specimens were collected after informed approval was received from the patients on the day of experiments. Participants engaged themselves in a completely voluntary approach, and they did not have any known pre-existing diseases at the time of participation. Each volunteer who participated in this study only provided one sample on a specific day.

## RESULTS AND DISCUSSIONS

**Mechanism of the Colorimetric Reaction.** The underlying chemical assay involves an Hgb-catalyzed redox reaction between 3,3'-dimethyl-[1,1'-biphenyl]-4,4'-diamine (o-tolidine) and hydrogen peroxide, generating a greenish-blue-colored product similar to the well-established and commercial assay protocol for spectrophotometric estimation of Hgb in plasma and other portable POC photometers.<sup>43–45</sup> We have optimized the reaction parameters to obtain quantifiable

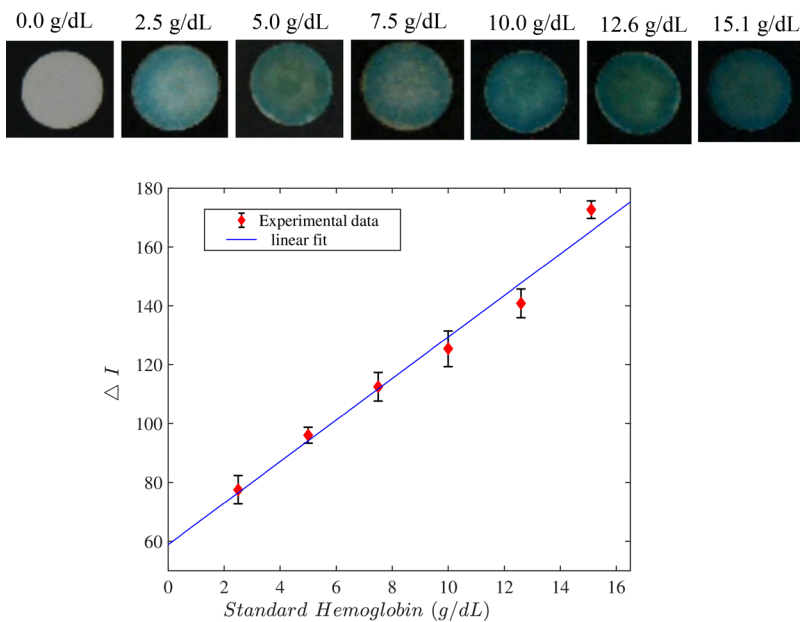


**Figure 4.** Standard calibration curve of the POC device for Hgb levels ranging from 2.5 to 15.1 g/dL ( $R = 0.9891$ , slope ( $m$ ) = 7.0557, and intercept ( $C$ ) = 58.843). The result was produced from images taken by a smartphone camera (as shown in the image at the top panel). Error bars represent standard deviations in the mean intensity computed from 20 trials corresponding to a specific concentration.

colorimetric signals to cover the entire physiological range of Hgb (5–18 g/dL) on a paper-based platform and thereby adopting the assay for rapid, reliable POC setting without requiring any ancillary equipment.

**Calibration Curve.** Reaction kinetics (Figure 3A) is depicted by the temporal variation of the normalized grayscale intensity obtained by

$$I_{\text{norm}}(t) = \frac{I_R(t) - I_{\text{UR}}}{I_{R,\text{MAX}} - I_{\text{UR}}} \quad (2)$$

Temporal variables  $I_{\text{norm}}(t)$ ,  $I_R(t)$ ,  $I_{R,\text{MAX}}$ , and  $I_{\text{UR}}$  denote the normalized intensity, the intensity of the reacted pad, the average intensity of saturated color, and the intensity of the unreacted pad, respectively.

Figure 3A illustrates reduction for the reaction completion time from a lower to a higher concentration of Hgb. From Figure 3B, it is evident that the reaction kinetics has three distinct phases where regime I signifies progression of chemical reaction till its completion. The regime (II) within the blue dotted lines is the temporally stable saturation region. The temporal average of the intensity in this region ( $I_{R,\text{MAX}}$ ) has been utilized for obtaining the calibrated intensity level ( $\Delta I$ ). In the decaying regime (III), the colorimetric signal gradually fades, which can be attributed to the intensity bleaching from the reaction pad. Differences of the scaled intensities ( $\Delta I$ ) are obtained for the specified concentrations as per eq 1. Mean and standard deviations corresponding to a set of experimental trials (repeated 20 runs for a given concentration) for each concentration are obtained and subsequently mapped with the specific concentrations as delineated in Figure 4.

**Assay Sensitivity.** To determine the sensitivity of the underlying chemical assay, i.e., the lowest limit of detection (LOD), we have performed the assay with standard hemoglobin solutions on our smartphone-enabled paper-based sensor. For this specific study, we detected hemoglobin of different known concentration values from 1.0 up to 7.0 g/dL. From Figure S4 in the Supporting Information, it is evident that the limit of

detection is 2.5 g/dL, below which the predictability is highly inconsistent as realized from the large error bars, though there is a distinct color generation even in the case of the lowest Hgb concentration studied (i.e., 1.0 g/dL). As per technical specification of a commonly used point-of-care device (i.e., HemoCue 201+) and standard hematology analyzer (i.e., Sysmex Kx21), both the devices are capable of detecting a wide range of Hgb concentrations, covering entire the range between 0 and 20 g/dL successfully.<sup>46,47</sup> However, determining the Hgb concentration in the lower range (specifically below 3.0 g/dL) is always challenging as these measurements accompany significant uncertainties. In a practical diagnostic scenario, finding patient samples below the Hgb concentration 3.0 g/dL is a very rare occurrence; thus, we believe that the LOD of our paper-based POC sensor is at par with the two devices that we used for comparison. Moreover, the machine learning-enabled feedback algorithm in our analysis will minimize the prediction errors (especially in the low Hgb range) as more test data will be recorded from future experiments.

**Demographic Characteristics of the Tested Samples.** In total, we have validated our paper-based sensor with 200 venous blood and 142 finger-prick blood samples collected from different volunteers at different courses of time. The demographic characteristics of the blood sample depict that majority of the participants were females (74.8% for venous blood and 72% for finger pricked blood) (Supporting Information, Table S1). Further derivation of these blood samples shows that the percentage of female samples tested was 100% for severely anemic ( $n = 9$ ) cases and 96.5% for mildly anemic ( $n = 79$ ) cases. The range of the age group of the participants was between 20 and 65 years for venous samples and 20 and 60 years for finger-pricked samples.

**Validation of the POC Device.** We have successfully validated our device with 200 venous blood (Figure 5) and 142 finger-pricked blood samples (Figure 6), covering the entire physiological range of Hgb concentration. The collected samples were stored in anti-coagulant-coated vials (k3EDTA 2

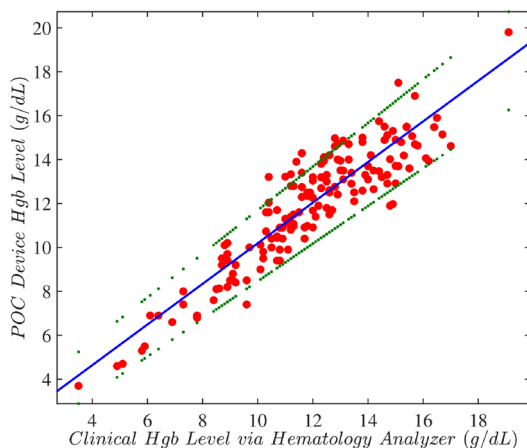


**Figure 5.** Clinical validations of POC outcomes in laboratory settings. POC results are put against clinical estimates (measured through a hematology analyzer) for  $n = 200$  (venous blood),  $R = 0.9583$ . Furthermore, 95% prediction limits for the individual values were shown by the dashed lines.

mL tubes) in room temperature prior to use for testing. However, the finger-pricked samples were tested immediately after drawing of the blood drop and directly introducing the drop onto the paper device (the test protocol is outlined in the Supporting Information). Figure 5 depicts the estimated Hgb levels against the values determined by a standard hematology analyzer, showing a strong correlation ( $r = 0.9583$ ,  $n = 200$ ).

The result of the POC device using finger-pricked blood samples shows good consistencies ( $r = 0.83$ ,  $n = 142$ ) (as shown in Figure 6A) with another well-known commercially available POC testing device, Hemocue HB-201+. We have successfully performed four field trials in rural settings in four different villages in the state of West Bengal, India (details of sample size variations are shown in Figure 6B), where minimally skilled frontline workers, with a brief training, conducted the entire test procedures. Further, environmental conditions were quite adverse during these field trials with extreme dirt, dust, high humidity (>70%), and soaring temperature (>36 °C) in comparison to the controlled conditions in standard laboratory environments. From the published literature, it is evident that the results of the Hemocue device vary between  $\pm 2.5$  g/dL

during a repeatability test.<sup>48</sup> The reproducibility of our device shown in the Supporting Information, Figure S2, is in the similar range and more precise. Colorimetric outcomes are plotted corresponding to the clinical Hgb levels measured via a hematology analyzer, while the error bars depict the standard deviation in the mean intensity obtained from five repeated runs of the experiment corresponding to a specific sample. Results from our paper-based sensor lie within a 10% coefficient of variation (CV) limit for 95% of the sample populations.

We have performed the assays in two different settings: (I) chromogenic reagents added on the reaction spots on site, i.e., ~15 min before adding the sample specimens, and (II) with pre-stored chromogenic reagents. The performance of the assays with pre-stored reagents remains unaltered up to 8 h while stored in room temperature (details provided in Figure S5 in the Supporting Information). For the field experiments, we have used the first strategy, i.e., adding the chromogenic reagents on site, i.e., 15 min before the assay was conducted.

The result from field trial 1 to field trial 4 shows continuous improvement toward precise estimation of the blood hemoglobin level using finger-pricked blood (Figure 7). The machine learning-based adaptive algorithm takes the device-tested results for identifying the difference with gold standard results and optimizes the best fit for next sets of calibration data after predictive computation. The result of the device further demonstrates the potential to be considered as an alternative diagnostic approach, which can improve the landscape of rural healthcare.

Further, to understand the commercial competitiveness of the POC device, we provide an approximate cost estimation per unit test (Supporting Information, Table S2). The whole procedure involves one-time remittance of a smartphone (~120 US \$), a plastic box with electronic components (~10 US \$ if it is outsourced for manufacturing), and the recurring costs of paper strips and chemical reagents. Considering that many users will have a pre-owned mobile phone in which the Sens-Hb app could be installed for free, the average expenses per test are estimated to be around 0.02 US \$ (excluding the expenses related to testing personnel, intellect, and institutional infrastructures), which is ~99% less expensive than the commercial cuvettes used in the HemoCue device. The overall cost can be reduced further if adopted for mass-scale manufacturing. The ease of disposal

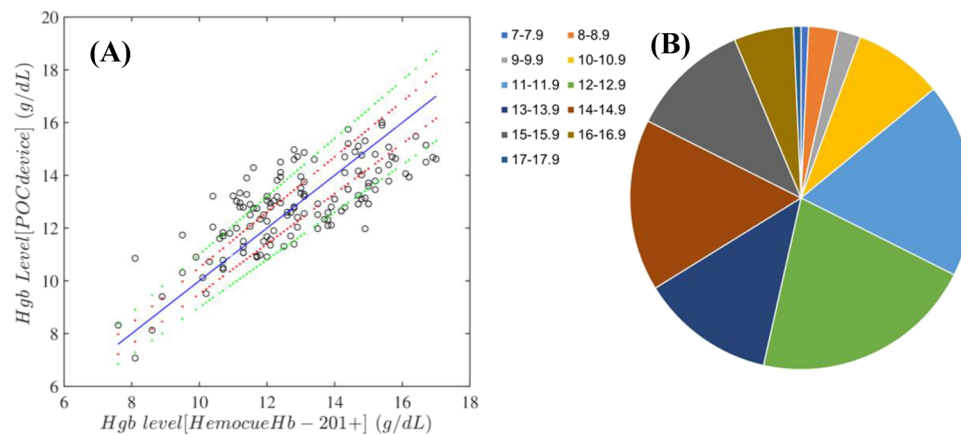


**Figure 6.** (A) Field results are plotted against the measurements obtained using the commercial POC testing platform (Hemocue HB-201+) for  $n = 142$  (finger-pricked blood),  $R = 0.83$  (5 and 10% deviations are shown through red and green lines, respectively). It is important to note that for only seven cases the results are wrongly predicted (mildly anemic cases are predicted in the healthy range with respect to the prediction made by the Hemocue device). (B) Distribution of sample size tested during the four field trials is shown in the pie chart.

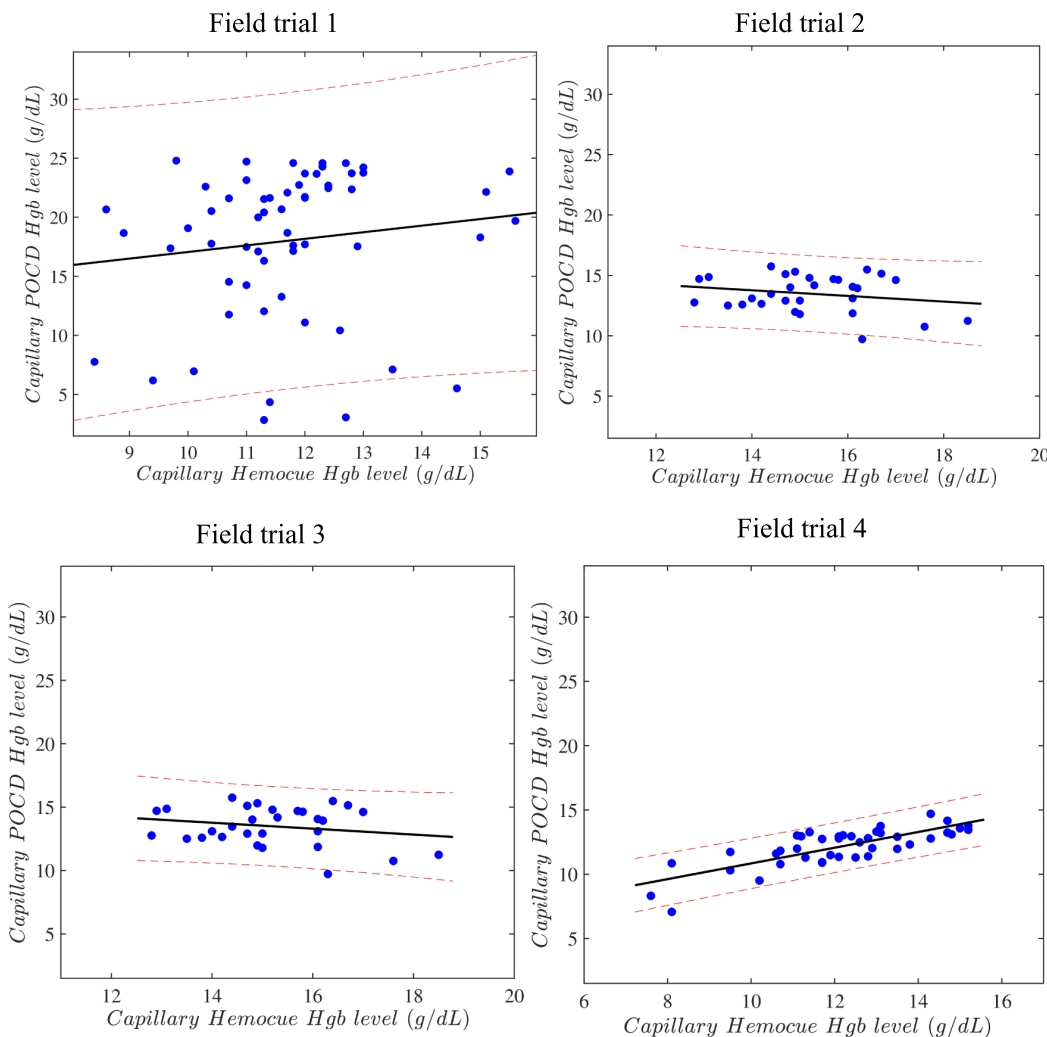


**Figure 7.** Results of four different field trials demonstrate the improvement in result accuracy from the first field trial to the fourth field trial. The usage of field validation results for adaptation of the calibration data set by the machine learning algorithm consistently narrows down the gap between the results obtained by our device and Hemocue Hb-201+.

(through burning) makes it further convenient for use in rural settings without requiring any intricate waste management strategies. Successful field trials with complete support from minimally trained frontline workers have been testimonial to establish the user friendliness of the testing method, obviating the involvement of trained laboratory personnel.

## CONCLUSIONS

In summary, we report a paper-based POC-sensing platform integrated with a smartphone application for quantitative estimation of Hgb. The device has been tested extensively both in the laboratory and field settings at extreme point of care. The variation in colorimetric signals generated from the reaction for low to high Hgb concentrations is clearly perceptible and discernible. Integration of a smartphone-based app obviates extensive manual interventions during the test and completes the entire diagnosis within 5 min. To improve the overall accuracy of the diagnosis, the validated outcomes are continuously adapted within the algorithm as new training data sets for recalibration. Our test results exhibit good correlation with the outcome of an automated hematology analyzer ( $r = 0.9583$ ) (Figure 5) and yielded comparable sensitivity and specificity for detecting mild anemia ( $n = 55$ )

(<11 g/dL) (sensitivity: 87.5%, specificity: 100%) and severe anemia ( $n = 9$ ) (<7 g/dL) (sensitivity: 100%, specificity: 100%), at par with other POC testing platforms. Difference in results of our POC device from the pathological estimates lies within the range of 0.5 g/dL for all severely anemic samples ( $n = 9$ ) and < 1.5 g/dL for the rest of the samples.

It is important to note the comparative advantages with respect to the widely used WHO hemoglobin color scale, which compares the color of a blood spot on paper with reference standards ranging from 4 to 14 g/dL in intervals of 2 g/dL to quantify Hgb levels.<sup>49,50</sup> In laboratory settings, this color scale offers 95% agreement within the limits of -3.50 to +3.11 g/dL.<sup>51</sup> Van Den Broek et al. reported that the color scale yielded quantitative measurements within 2 g/dL for only 67% of the samples.<sup>52</sup> In this context, the present paper-based sensor offers a robust, accurate and yet affordable diagnostic approach, which can be adopted in rural settings to facilitate decentralized healthcare facilities, and holds the promises of replacing the WHO colorimetric scale without any cost penalty.

## ■ ASSOCIATED CONTENT

### SI Supporting Information

The Supporting Information is available free of charge at <https://pubs.acs.org/doi/10.1021/acssensors.0c02361>.

(Figure S1) Detection Steps of the smartphone application; Preparation of Chromogenic reagent; RReliefF algorithm for feature selection; (Table S1) baseline demographic and clinical characteristics of participants; (Figure S2) repeatability test of the device and estimation of coefficient of variation; (Table S2) cost-break-up per test; (Figure S3) images of clinical field trials; (Figure S4) determination of the limit of detection; and (Figure S5) impact of reagent storage on the paper sensor ([PDF](#))

Sens-Hb detection video showing the stepwise testing protocol for field experiments ([MP4](#))

## ■ AUTHOR INFORMATION

### Corresponding Author

Suman Chakraborty – Department of Mechanical Engineering and Advanced Technology Development Centre, Indian Institute of Technology Kharagpur, Kharagpur 721302, India; [ORCID.org/0000-0002-5454-9766](https://orcid.org/0000-0002-5454-9766); Phone: +91-3222-282990; Email: [suman@mech.iitkgp.ac.in](mailto:suman@mech.iitkgp.ac.in)

### Authors

Sujay K. Biswas – School of Medical Science and Technology, Indian Institute of Technology Kharagpur, Kharagpur 721302, India

Subhamoy Chatterjee – Electronics and Electrical Communication Engineering, Indian Institute of Technology Kharagpur, Kharagpur 721302, India

Soumya Bandyopadhyay – Department of Mechanical Engineering, Indian Institute of Technology Kharagpur, Kharagpur 721302, India

Shantimoy Kar – Advanced Technology Development Centre, Indian Institute of Technology Kharagpur, Kharagpur 721302, India; Currently working as a postdoctoral research assistant in the University of Glasgow, Glasgow G12 8LT, U.K.

Nirmal K. Som – BC Roy Technology Hospital, Indian Institute of Technology Kharagpur, Kharagpur 721302, India

Satadal Saha – School of Medical Science and Technology, Indian Institute of Technology Kharagpur, Kharagpur 721302, India; BC Roy Institute of Medical Science and Research, Indian Institute of Technology Kharagpur, Kharagpur 721302, India; JSV Innovations Pvt. Ltd, Kolkata 700025, India

Complete contact information is available at:

<https://pubs.acs.org/10.1021/acssensors.0c02361>

### Notes

The authors declare no competing financial interest.

## ■ ACKNOWLEDGMENTS

We appreciate the collaborative support from BC Roy Technology Hospital, Indian Institute of Technology for collection of blood samples and for sharing the pathological test results. Further, we acknowledge JSV Innovation Pvt. Ltd. for facilitating us to carry out joint field trial activities at their health KIOSKS in rural Indian villages in the state of West Bengal. This work is a part of the project entitled “Development of Smartphone Integrated Generic Microfluidic Devices for

Rapid, Portable and Affordable Point-of-Care Diagnostics”, jointly funded by a grant from the Ministry of Human Resource Development (MHRD) and Indian Council of Medical Research (ICMR), Department of Health Research, Ministry of Health and Family Welfare, New Delhi, as a part of the IMPRINT Programme. Additional research support has been provided by the Ministry of Electronics and Information Technology (MEITY), Government of India. S.C. acknowledges financial support from the Department of Science and Technology, Government of India, through the Sir J.C. Bose National Fellowship.

## ■ REFERENCES

- (1) Yang, X.; Piety, N. Z.; Vignes, S. M.; Benton, M. S.; Kanter, J.; Shevkoplyas, S. S. Simple Paper-Based Test for Measuring Blood Hemoglobin Concentration in Resource-Limited Settings. *Clin. Chem.* **2013**, *59*, 1506–1513.
- (2) Grammer, T. B.; Scharnagl, H.; Dressel, A.; Kleber, M. E.; Silbernagel, G.; Pilz, S.; Tomaschitz, A.; Koenig, W.; Mueller-Myhsok, B.; März, W.; Strnád, P. Iron Metabolism, Hepcidin, and Mortality (the Ludwigshafen Risk and Cardiovascular Health Study). *Clin. Chem.* **2019**, *65*, 849–861.
- (3) Vos, T.; Allen, C.; Arora, M.; Barber, R. M.; Brown, A.; Carter, A.; Zuhlké, L. J. Global, Regional, and National Incidence, Prevalence, and Years Lived with Disability for 310 Diseases and Injuries, 1990–2015: A Systematic Analysis for the Global Burden of Disease Study 2015. *Lancet* **2016**, *388*, 1545–1602.
- (4) World Health Organization 2015. The Global Prevalence of Anaemia in 2011. *WHO Report* **2011**, 48.
- (5) McLean, E.; Cogswell, M.; Egli, I.; Wojdyla, D.; De Benoist, B. Worldwide Prevalence of Anaemia, WHO Vitamin and Mineral Nutrition Information System, 1993–2005. *Public Health Nutr.* **2009**, *12*, 444–454.
- (6) Eilers, R. J. Notification of Final Adoption of an International Method and Standard Solution for Hemoglobinometry Specifications for Preparation of Standard Solution. *Am. J. Clin. Pathol.* **1967**, *47*, 212–214.
- (7) Van Kampen, E. J.; Zijlstra, W. G. Standardization of Hemoglobinometry II. The Hemiglobincyanide Method. *Clin. Chim. Acta* **1961**, *6*, 538–544.
- (8) Agarwal, R.; Sarkar, A.; Bhowmik, A.; Mukherjee, D.; Chakraborty, S. A Portable Spinning Disc for Complete Blood Count (CBC). *Biosens. Bioelectron.* **2020**, *150*, 111935.
- (9) Kar, S.; Ghosh, U.; Maiti, T. K.; Chakraborty, S. Haemoglobin Content Modulated Deformation Dynamics of Red Blood Cells on a Compact Disc. *Lab Chip* **2015**, *15*, 4571–4577.
- (10) Guo, J. Smartphone-Powered Electrochemical Biosensing Dongle for Emerging Medical IoTs Application. *IEEE Transactions on Industrial Informatics* **2018**, *14*, 2592–2597.
- (11) Guo, J. Smartphone-Powered Electrochemical Dongle for Point-of-Care Monitoring of Blood  $\beta$ -Ketone. *Anal. Chem.* **2017**, *89*, 8609–8613.
- (12) Guo, J. Uric Acid Monitoring with a Smartphone as the Electrochemical Analyzer. *Anal. Chem.* **2016**, *88*, 11986–11989.
- (13) Li, B.; Qi, J.; Fu, L.; Han, J.; Choo, J.; DeMello, A. J.; Lin, B.; Chen, L. Integrated Hand-Powered Centrifugation and Paper-Based Diagnosis with Blood-in/Answer-out Capabilities. *Biosens. Bioelectron.* **2020**, *165*, 112282.
- (14) Ki, H.; Jang, H.; Oh, J.; Han, G.-R.; Lee, H.; Kim, S.; Kim, M.-G. Simultaneous Detection of Serum Glucose and Glycated Albumin on a Paper-Based Sensor for Acute Hyperglycemia and Diabetes Mellitus. *Anal. Chem.* **2020**, *92*, 11530–11534.
- (15) Tan, W.; Zhang, L.; Doery, J. C. G.; Shen, W. Study of Paper-Based Assaying System for Diagnosis of Total Serum Bilirubin by Colorimetric Diazotization Method. *Sens. Actuators, B* **2020**, *305*, 127448.
- (16) Tan, W.; Zhang, L.; Doery, J. C. G.; Shen, W. Three-Dimensional Microfluidic Tape-Paper-Based Sensing Device for Blood Total

- Bilirubin Measurement in Jaundiced Neonates. *Lab Chip* **2020**, *20*, 394–404.
- (17) Sun, X.; Li, B.; Tian, C.; Yu, F.; Zhou, N.; Zhan, Y.; Chen, L. Rotational Paper-Based Electrochemiluminescence Immunodevices for Sensitive and Multiplexed Detection of Cancer Biomarkers. *Anal. Chim. Acta* **2018**, *1007*, 33–39.
- (18) Qi, J.; Li, B.; Zhou, N.; Wang, X.; Deng, D.; Luo, L.; Chen, L. The Strategy of Antibody-Free Biomarker Analysis by in-Situ Synthesized Molecularly Imprinted Polymers on Movable Valve Paper-Based Device. *Biosens. Bioelectron.* **2019**, *142*, 111533.
- (19) Fu, Y.; Yan, M.; Yang, H.; Ma, X.; Guo, J. Palm-Sized Uric Acid Test Lab Powered by Smartphone for Proactive Gout Management. *IEEE Transactions on Biomedical Circuits and Systems* **2019**, *13*, 950–956.
- (20) Guo, J.; Huang, X.; Ma, X. Clinical Identification of Diabetic Ketosis/Diabetic Ketoacidosis Acid by Electrochemical Dual Channel Test Strip with Medical Smartphone. *Sens. Actuators, B* **2018**, *275*, 446–450.
- (21) Kaiho, S. i.; Mizuno, K. Sensitive Assay Systems for Detection of Hemoglobin with 2,7-Diaminofluorene: Histochemistry and Colorimetry for Erythrodifferentiation. *Anal. Biochem.* **1985**, *149*, 117–120.
- (22) Toh, R. J.; Peng, W. K.; Han, J.; Pumera, M. Direct in Vivo Electrochemical Detection of Haemoglobin in Red Blood Cells. *Sci. Rep.* **2014**, *4*, 1–6.
- (23) Barati, A.; Shamsipur, M.; Abdollahi, H. Hemoglobin Detection Using Carbon Dots as a Fluorescence Probe. *Biosens. Bioelectron.* **2015**, *71*, 470–475.
- (24) Wang, X.; Yu, S.; Liu, W.; Fu, L.; Wang, Y.; Li, J.; Chen, L. Molecular Imprinting Based Hybrid Ratiometric Fluorescence Sensor for the Visual Determination of Bovine Hemoglobin. *ACS Sensors* **2018**, *3*, 378–385.
- (25) Shajaripour Jaber, S. Y.; Ghaffarinejad, A.; Omidinia, E. An Electrochemical Paper Based Nano-Genosensor Modified with Reduced Graphene Oxide-Gold Nanostructure for Determination of Glycated Hemoglobin in Blood. *Anal. Chim. Acta* **2019**, *1078*, 42–52.
- (26) Yang, Q.; Li, J.; Wang, X.; Xiong, H.; Chen, L. Ternary Emission of a Blue-, Green-, and Red-Based Molecular Imprinting Fluorescence Sensor for the Multiplexed and Visual Detection of Bovine Hemoglobin. *Anal. Chem.* **2019**, *91*, 6561–6568.
- (27) Taparia, N.; Platten, K. C.; Anderson, K. B.; Sniadecki, N. J. A Microfluidic Approach for Hemoglobin Detection in Whole Blood. *AIP Adv.* **2017**, *7*, 105102–105111.
- (28) Hasan, M. N.; Fraiwan, A.; An, R.; Alapan, Y.; Ung, R.; Akkus, A.; Xu, J. Z.; Rezac, A. J.; Kocmich, N. J.; Creary, M. S.; Oginni, T.; Olanipekun, G. M.; Hassan-Hanga, F.; Jibir, B. W.; Gambo, S.; Verma, A. K.; Bharti, P. K.; Rioulueang, S.; Ngimhung, T.; Suksangpleng, T.; Thota, P.; Werner, G.; Shanmugam, R.; Das, A.; Viprakasit, V.; Piccone, C. M.; Little, J. A.; Obaro, S. K.; Gurkan, U. A. Paper-Based Microchip Electrophoresis for Point-of-Care Hemoglobin Testing. *Analyst* **2020**, *145*, 2525–2542.
- (29) Kar, S.; Das, S. S.; Laha, S.; Chakraborty, S. Microfluidics on Porous Substrates Mediated by Capillarity-Driven Transport. *Ind. Eng. Chem. Res.* **2020**, *59*, 3644–3654.
- (30) Kar, S.; Chakraborty, S. Evolution of Paper Microfluidics as an Alternate Diagnostic Platform. In *Paper Microfluidics: Theory and Applications*. Bhattacharya, S., Kumar, S., Agarwal, A. K., Eds., Springer: Singapore 2019, 83–98, DOI: 10.1007/978-981-15-0489-1\_6.
- (31) Kar, S.; Maiti, T. K.; Chakraborty, S. Capillarity-Driven Blood Plasma Separation on Paper-Based Devices. *Analyst* **2015**, *140*, 6473–6476.
- (32) Dey, R.; Kar, S.; Joshi, S.; Maiti, T. K.; Chakraborty, S. Ultra-Low-Cost ‘Paper-and-Pencil’ Device for Electrically Controlled Micro-mixing of Analytes. *Microfluid. Nanofluid.* **2015**, *19*, 375–383.
- (33) Han, J.; Qi, A.; Zhou, J.; Wang, G.; Li, B.; Chen, L. Simple Way To Fabricate Novel Paper-Based Valves Using Plastic Comb Binding Spines. *ACS Sensors* **2018**, *3*, 1789–1794.
- (34) Lu, Y.; Shi, W.; Qin, J.; Lin, B. Fabrication and Characterization of Paper-Based Microfluidics Prepared in Nitrocellulose Membrane By Wax Printing. *Anal. Chem.* **2010**, *82*, 329–335.
- (35) Matsuura, K.; Chen, K.-H.; Tsai, C.-H.; Li, W.; Asano, Y.; Naruse, K.; Cheng, C.-M. Paper-Based Diagnostic Devices for Evaluating the Quality of Human Sperm. *Microfluid. Nanofluid.* **2014**, *16*, 857–867.
- (36) Chen, C.; Lin, B. R.; Wang, H. K.; Fan, S. T.; Hsu, M. Y.; Cheng, C. M. Paper-Based Immunoaffinity Devices for Accessible Isolation and Characterization of Extracellular Vesicles. *Microfluid. Nanofluid.* **2014**, *16*, 849–856.
- (37) Mani, N. K.; Prabhu, A.; Biswas, S. K.; Chakraborty, S. Fabricating Paper Based Devices Using Correction Pens. *Sci. Rep.* **2019**, *9*, 1752.
- (38) Mandal, P.; Dey, R.; Chakraborty, S. Electrokinetics with “Paper-and-Pencil” Devices. *Lab Chip* **2012**, *12*, 4026.
- (39) Robnik-Sikonja, M.; Kononenko, I. An Adaptation of {R}elief for Attribute Estimation in Regression. In *Machine Learning: Proceedings of the Fourteenth International Conference (ICML'97)*; 1997; pp. 296–304.
- (40) Jia, J.; Yang, N.; Zhang, C.; Yue, A.; Yang, J.; Zhu, D. Object-Oriented Feature Selection of High Spatial Resolution Images Using an Improved Relief Algorithm. *Mathematical and Computer Modelling* **2013**, *58*, 619–626.
- (41) Urbanowicz, R. J.; Meeker, M.; La Cava, W.; Olson, R. S.; Moore, J. H. Relief-Based Feature Selection: Introduction and Review. *Journal of Biomedical Informatics* **2018**, *85*, 189–203.
- (42) Urbanowicz, R. J.; Olson, R. S.; Schmitt, P.; Meeker, M.; Moore, J. H. Benchmarking Relief-Based Feature Selection Methods for Bioinformatics Data Mining. *Journal of Biomedical Informatics* **2018**, *85*, 168–188.
- (43) Goyal, M. M.; Basak, A. Estimation of Plasma Haemoglobin by a Modified Kinetic Method Using O-Tolidine. *Indian Journal of Clinical Biochemistry* **2009**, *24*, 36–41.
- (44) Tyburski, E. A.; Lyon, L. A.; Lam, W. A. Disposable Platform Provides Visual and Color- Based Point-of-Care Anemia Self-Testing Find the Latest Version : Disposable Platform Provides Visual and Color-Based Point-of-Care Anemia Self-Testing. **2014**, *124* (10), 4387–4394, DOI: 10.1172/JCI76666.
- (45) McMurdy, J. W.; Jay, G. D.; Suner, S.; Crawford, G. Noninvasive Optical, Electrical, and Acoustic Methods of Total Hemoglobin Determination. *Clin. Chem.* **2008**, *54*, 264–272.
- (46) Hemocue. *HemoCue® Hb 201+ System*. Available at Hemocue Website: <https://www.hemocue.in/en-in/solutions/hematology/hemocue-hb-201plus-system>.
- (47) Hamaguchi, Y.; Tamiaki, K.; Nakai, R.; Ochi, Y.; Okazaki, T.; Uchihashi, K.; Morikawa, T. Overview and Features of the Automated Hematology Analyzer. *Sysmex Journal International* **2015**, *25*, 1–12.
- (48) Patel, A. J.; Wesley, R.; Leitman, S. F.; Bryant, B. J. Capillary versus Venous Haemoglobin Determination in the Assessment of Healthy Blood Donors. *Vox Sang.* **2013**, *104*, 317–323.
- (49) Critchley, J.; Bates, I. Haemoglobin Colour Scale for Anaemia Diagnosis Where There Is No Laboratory: A Systematic Review. *Int. J. Epidemiol.* **2005**, *34*, 1425–1434.
- (50) Lewis, S. M.; Stott, G. J.; Wynn, K. J. An Inexpensive and Reliable New Haemoglobin Colour Scale for Assessing Anaemia. *J. Clin. Pathol.* **1998**, *51*, 21–24.
- (51) Paddle, J. J. Evaluation of the Haemoglobin Colour Scale and Comparison with the HemoCue Haemoglobin Assay. *Bull. W. H. O.* **2002**, *80*, 813–816.
- (52) Van Den Broek, N. R.; Ntonya, C.; Mhango, E.; White, S. A. Diagnosing Anaemia in Pregnancy in Rural Clinics: Assessing the Potential of the Haemoglobin Colour Scale. *Bull. W. H. O.* **1999**, *77*, 15–21.